Generation and characterization of a conditional deletion allele for *Lmna* in mice

Youngjo Kim, Yixian Zheng *

Department of Embryology, Carnegie Institution for Science, 3520 San Martin Dr., Baltimore, MD 21218, USA

ARTICLE INFO

ABSTRACT

Extensive efforts have been devoted to study A-type lamins because mutations in their gene, *LMNA* in humans, are associated with a number of diseases. The mouse germline mutations in the A-type lamins (encoded by *Lmna*) exhibit postnatal lethality at either 4–8 postnatal (P) weeks or P16–18 days, depending on the deletion alleles. These mice exhibit defects in several tissues including hearts and skeletal muscles. Despite numerous studies, how the germline mutation of *Lmna*, which is expressed in many postnatal tissues, affects only selected tissues remains poorly understood. Addressing the tissue specific functions of *Lmna* requires the generation and careful characterization of conditional *Lmna* null alleles. Here we report the creation of a conditional *Lmna* knockout allele in mice by introducing loxP sites flanking the second exon of *Lmna*. The *Lmna*flox/flox mice are phenotypically normal and fertile. We show that *Lmna* homozygous mutants (*Lmna*Δ/Δ) generated by germline Cre expression display postnatal lethality at P16–18 days with defects similar to a recently reported germline *Lmna* knockout mouse that exhibits the earliest lethality compared to other germline knockout alleles. This conditional knockout mouse strain should serve as an important genetic tool to study the tissue specific roles of *Lmna*, which would contribute toward the understanding of various human diseases associated with A-type lamins.

© 2013 Elsevier Inc. All rights reserved.

1. Introduction

The nuclear lamina (NL) is a meshwork of proteins that lines the inner nuclear membrane and serves as a nuclear scaffold. Lamins, which belong to the type V intermediate filaments, are the major components of the NL. Lamin proteins were initially subdivided based on immunological and biochemical criteria [1,2]. A-type lamins have nearly neutral isoelectric points (pI) and are almost completely solubilized during mitosis, whereas B-type lamins have acidic pI and remain associated with nuclear envelope derived membranes during mitosis. Since the first cDNA cloning of A-type lamins in humans [3], lamins have been identified in many vertebrates. Sequence comparisons of lamin proteins have revealed that despite of overall similarity, A- and B-type lamins exhibit subclass-specific sequence variations [4–6]. It is also known that both A and B-type lamins are initially carboxymethylated and farnesylated at the C-terminal CaaX motif, but these modifications are removed from lamin-A by proteolysis (reviewed in [7]).

In the mouse, *Lmnb1* and *Lmnb2* encode lamin-B1 and lamin-B2, respectively. *Lmnb2* also expresses lamin-B3 through alternatively splicing in the testes. On the other hand, *Lmna* expresses several forms of A-type lamins, including lamin-A, -C, -AΔ10, and -C2,

via alternative splicing. While B-type lamins are expressed in most cell types throughout development, the expression of A-type lamins is either lacking or very low during early development with increasing levels of expression in some cell types as development progresses [8–10]. For example, during mouse embryogenesis, the expression of A-type lamins is limited to a few tissues such as the trunk and epidermis, while in many other tissues, lamin-A/C is not detected until well after birth. In adult mice, lamin-A/C are expressed in many tissues at high levels [9].

Since the discovery that mutations in *LMNA* cause autosomal dominant Emery–Dreifuss muscular dystrophy (EDMD) in humans [11], many additional *LMNA* mutations have been shown to cause a large group of human diseases ranging from muscular dystrophy to premature aging disease. Several germline *Lmna* mutant mouse models have been generated with the aim of understanding the mechanisms by which A-type lamins function in health and diseases [12,13]. Sullivan and colleagues showed that homozygous mice deleted of exons 8–11 of *Lmna* (referred to here as *Lmna*Δ8–11/Δ8–11) in the germline develop to term with no overt abnormalities [14]. However, their postnatal growths are severely retarded, and these mice present with a subset of pathologies similar to those caused by *LMNA* mutations, including muscular dystrophy, dilated cardiomyopathy, and Charcot–Marie–Tooth syndrome in humans [15]. These mice die at around 4–8 weeks after birth. Despite the widespread use of this mouse

model, recent studies show that these mice still express a truncated lamin-A protein of 54 kDa, which corresponds to the 468 amino acids encoded by exons 1–7 and 12, through alternative splicing [16]. The expression of this large lamin-A fragment might function dominant negatively because heterozygous $Lmna^{+/\Delta 8-11}$ mice develop dilated cardiomyopathies 4 weeks after birth [17], which complicates phenotypic interpretation.

Recently, another *Lmna* germline knockout mouse line has been created using gene trap (GT) technology [13]. In the $Lmna^{GT-/-}$ mouse, a gene trap cassette, consisting of a splicing acceptor and a reporter gene, is introduced into the upstream sequence of exon 2 of *Lmna*, and only the N-terminal 118 amino acids of lamin-A is expressed as a fusion with the reporter protein. $Lmna^{GT-/-}$ mice are overtly normal during embryogenesis. However, they succumb to death at 16–18 days after birth, which is much earlier than $Lmna^{\Delta 8-11/\Delta 8-11}$ mice. Therefore, $Lmna^{GT-/-}$ mice are the most severe loss-of-function mutants for A-type lamins to date.

Although mutations of *LMNA* are associated with diverse human diseases, a careful look at the diseases and animal models reveals that the defects caused by different mutations are manifested in limited tissue types including striated muscles, adipose tissues, and peripheral nerves [18]. How mutations in the broadly expressed lamin-A cause tissue-restricted defects is unclear. Several nonexclusive hypotheses have been proposed to account for the molecular basis of this selectivity [19]. For example, the mechanical stress model posits that cell types such as muscle cells that are under constant mechanical stress might be more susceptible to the alteration of the nuclear lamina [20]. The gene expression model, on the other hand, proposes that lamins influence gene expression profiles in a cell type specific manner [21,22]. Although studies using the germline *Lmna* mutant mouse models created thus far have provided support to aspects of the above hypotheses, understanding the function of *Lmna* in a given tissue requires the creation of a conditional *Lmna* knockout allele. Recently, Solovei et al. reported the use of an *Lmna* conditional knockout allele, which leads to the deletion of the last three exons (exons 10–12) of *Lmna* upon Cre expression [23]. The predicted lack of polyA signal in *Lmna* transcripts from exons 1–9 may cause their degradation. However, these transcripts could utilize a cryptic polyA signal in the absence of exons 10–12, which would lead to the generation of truncated lamin-A/C proteins. Unfortunately, the authors provided no characterization of this *Lmna* conditional knockout allele. Thus it remains unclear whether truncated lamin-A/C proteins are present upon Cre expression in these mice. To facilitate the study of the tissue autonomous function of A-type lamins, we report the generation and characterization of a different conditional *Lmna* knockout mouse model that deletes the majority of lamin-A/C proteins upon Cre-mediated recombination.

2. Materials and methods

2.1. Construction of the targeting vector

The targeting vector to generate conditional knockout alleles of *Lmna* was constructed using the recombineering protocol established by the Capecchi laboratory [24]. Briefly, an 8 kb genomic region from 2 kb upstream of exon 2 through the middle of exon 11 of *Lmna* was retrieved from a mouse BAC clone RP24-265E18, and was cloned into the pStart-K vector using Red-recombinase mediated cloning method. The construct was modified to add the 5′ and 3′ loxP sites at 100 bp upstream and downstream, respectively, from exon 2 of *Lmna* by a series of conventional and recombination-mediated cloning. The resulting plasmid was cut between exon 2 and the 3′ loxP site with the restriction enzyme MluI and

ligated to an Frt-puro-Frt cassette flanked by MluI sites to obtain a positive selection marker. Finally, the modified genomic fragment of *Lmna* in the pStart-K vector was transferred by Gateway recombination to the pWS-TK6 vector containing a thymidine kinase (tk) cassette as a negative selection marker. Full DNA sequences of the *Lmna* targeting vector were verified by conventional DNA sequencing, and are available upon request. All procedures involving recombinant DNA have followed the National Institute of Health guidelines.

2.2. PCR primers and mouse strains

To generate the $Lmna^{fflox}$ allele, the *Lmna* targeting vector was linearized by AsiSI and introduced into V6.5 mouse ESCs by electroporation. After selection with 1 µg/ml puromycin (Life Technologies) and 2 µM ganciclovir (Sigma, G2536), ESC clones were screened for homologous recombination by long-range PCR of the flanking regions of the 5′ and 3′ recombination arms from the genomic DNA. The PCR primers used to screen for the homologously recombined ESC clones are as follows:

P1F: 5′-GAGAGTGTGAGAATGTCAGCTTAGAC-3′
P1R: 5′-TTTCTAGAGAATAGGAACTTCACGCG-3′
P2F: 5′-GGCTCTATGGCTTCTGAGGCGGAAAG-3′
P2R: 5′-TCCCGCTCCACCGGCAGCCTTGTCAG-3′

To generate $Lmna^{flox}$ allele in which the puromycin cassette flanked by Frt sites is deleted, $Lmna^{fflox/+}$ mice were bred with ACTB-FLPe mice (#003800, JAX lab), which express a variant of FLP1 recombinase with enhanced thermal stability in a wide variety of tissues including germ cells. $Lmna^{flox/+}$ mice were identified by PCR of the flanking region of exon 2 of *Lmna*. PCR primers used to genotype all possible *Lmna* alleles in the resulting offspring are as follows:

P3F: 5′-AACCCAGCCTCAGAAACTGGTGGATG-3′
P3R: 5′-GACAGCTCTCCTCTGAAGTGCTTGGA-3′

$Lmna^{flox/+}$ mice were intercrossed to generate $Lmna^{flox/flox}$ mice, and maintained in a mixed genetic background from CD1, 129 Sv, and C57Bl/6 J strains.

To generate the $Lmna^{\Delta}$ allele, $Lmna^{flox/+}$ mice were bred with CMV-Cre mice (#003465, JAX lab). The generation of $Lmna^{\Delta}$ allele in the F1 generation of $Lmna^{flox/+} \times$ CMV-Cre mating pairs were screened by PCR of tail DNA with the primer pair P3F/R. CMV-Cre allele was genotyped according to the PCR protocol for generic Cre from the Jackson Laboratory. To remove the CMV-Cre allele present in the F1 generation, $Lmna^{\Delta/+}$; CMV-Cre$^{+/-}$ mice were outcrossed with 129S6/SvEvTac (Taconic). $Lmna^{\Delta/+}$ mice in the F2 generation that lacked the CMV-Cre allele were used to generate the $Lmna^{\Delta/\Delta}$ mice analyzed in this study. $Lmna^{+/+}$, $Lmna^{\Delta/+}$, and $Lmna^{\Delta/\Delta}$ mice were genotyped by PCR with the primer pair P3F/R. Mice used in this study are available upon request.

2.3. Isolation of MEFs

MEFs were generated by a standard protocol. Briefly, embryos were collected from the uteri of pregnant mice at embryonic day 13.5. The heads, visceral tissues and gonads of embryos were removed. The remaining embryonic bodies were minced and trypsinized twice. Fibroblasts from each embryo were harvested by centrifugation and then plated in MEF medium [15% FBS, 100 µM β-mercaptoethanol, 2 mM ʟ-glutamine, 0.1 mM nonessential amino acids, 1 mM sodium pyruvate, 50 µg/ml penicillin/streptomycin in Knockout DMEM (Life Technologies)]. Passage 1 MEFs were used for immunofluorescence staining and Western blotting analysis. Genomic DNA isolated from embryo heads were used for PCR genotyping.

2.4. Antibodies, Western blotting, and immunofluorescence staining

Western blotting analysis was performed as described [25]. Monoclonal mouse anti-lamin-A/C (Active Motif 39,287, 1:1000), goat anti-lamin-B1 (Santa Cruz sc-6216, 1:200), and monoclonal mouse anti-α-tubulin (Sigma T9026, 1:5000) were used as the primary antibodies. The monoclonal anti-lamin-A/C antibody used in this study was raised against a recombinant protein corresponding to amino acids 430–545 of human Lamin-A. Anti-mouse IgG HRP and anti-goat IgG HRP (Pierce) were used as secondary antibodies. Immunofluorescence staining was performed as described [25]. Mouse anti-lamin-A/C (Active Motif 39,287, 1:1000) and donkey anti-mouse IgG DyLight 488 were used as primary and secondary antibodies, respectively.

2.5. Histology

Tibialis anterior (TA) muscles were dissected from 15 day old mice, snap frozen, and sectioned at 10 μm thickness by a Leica CM3000 Cryostat. Sectioned TA muscles were used for either immunofluorescence staining for lamin-A/C or haematoxylin and eosin (H&E) staining after washing with PBS. Immunofluorescence and H&E staining were performed as described [25].

2.6. Quantitation of myofibril size

Cross-sectioned TA muscles were stained by H&E. Digital images were acquired with a CCD camera by routine bright field microscopy. Myofibrils were individually delineated by Photoshop software, and the area of each myofibril was determined by counting pixels. To convert to μm² units, pixel numbers of myofibrils were normalized by those of unit area measured by the scale bar.

3. Results and discussion

3.1. Generation of Lmna^fflox/+, Lmna^flox/+, and Lmna^flox/flox mice

Wild-type Lmna allele consists of 12 exons, which encode 665 amino acids, and an alternative first exon, 1c, that contributes to 7 amino acids at the N-terminus of lamin-C2 (Fig. 1A). Exon 1 and 1c of Lmna are separated by an intronic region of over 9 kb, which could make the deletion of the two exons inefficient. This would be undesirable for a conditional allele. Therefore, to remove all isoforms of lamin-A including lamin-C2, we set out to create a conditional exon 2 deletion allele. We constructed a targeting vector in which exon 2 of Lmna is flanked by loxP and Frt-Puro-Frt-loxP (Fig. 1B). The Lmna targeting vector was introduced into the V6.5 mouse embryonic stem cells (ESC) to replace exon 2 of Lmna with the chimeric sequences in the vector by homologous recombination (Fig. 1A and B). After positive and negative selections with puromycin and ganciclovir, respectively, we screened ESC clones for homologous recombination at both the 5′ and 3′ arms by long-range PCR using the P1F/R and P2F/R primer pairs (data not shown). We named this allele, which still has Frt-puro-Frt cassette, as Lmna^fflox (Fig. 1C) to distinguish it from the further processed Lmna alleles.

The selected ESC clone containing the Lmna^fflox allele was injected into blastocysts to generate chimeras as previously described [25]. Male chimeras were bred with CD1 females to
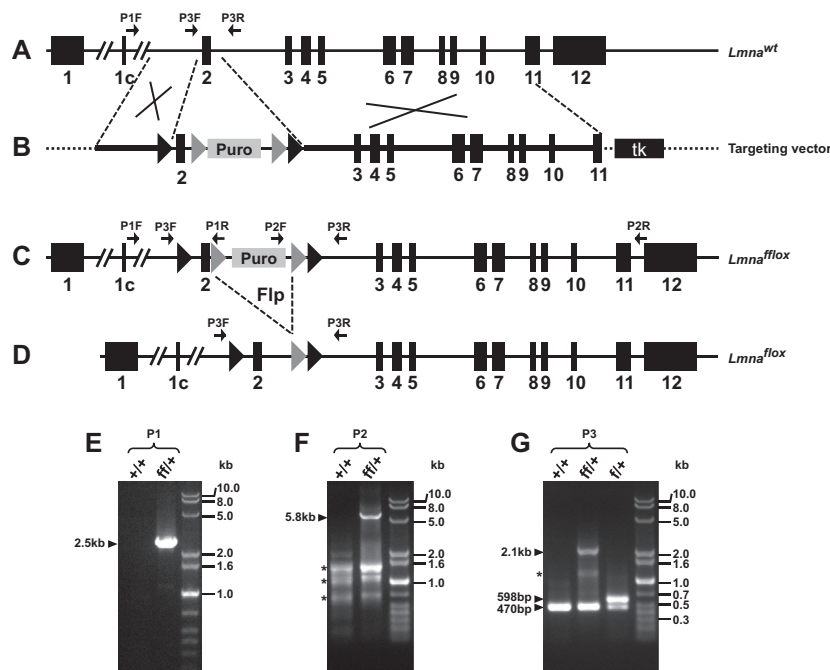
Fig. 1. Generation of Lmna conditional knockout alleles. (A–D) Targeting and breeding strategies. A 357 bp fragment from 100 bp upstream through 100 bp downstream of exon 2 of Lmna (A) was replaced with the chimeric sequences in the targeting vector (B) by homologous recombination to delete exon 2 upon expression of Cre recombinase. To generate the Lmna^fflox allele (C), the Lmna targeting vector was introduced into V6.5 ESCs. After screening for homologous recombination, Lmna^fflox/+ ESCs were injected into CD1 blastocysts to generate Lmna^fflox/+ mice. Lmna^fflox/+ mice were bred with a mouse strain expressing FLP1 recombinase to generate the Lmna^flox allele in which the Frt-puro-Frt cassette is cleaved (D). Exons are represented as boxes. Thick lines demarcated by dashed lines in the targeting vector indicate the targeting arms corresponding to the genomic regions in the Lmna gene. Large black and gray arrow heads represent the loxP and Frt sites, respectively. Puro, puromycin resistance gene; tk, thymidine kinase gene; Flp, FLP1 recombinase (flippase). (E and F) Confirmation of homologous recombination of the 5′ (E) and 3′ (F) arms in the Lmna^fflox allele. (E) Correct homologous recombination of the 5′ arms is indicated by the amplification of 2471 bp PCR fragments from the Lmna^fflox allele. (F) Correct homologous recombination of the 3′ arms is indicated by the amplification of 5817 bp PCR fragments from the Lmna^fflox allele. (G) PCR genotyping of the Lmna alleles with the P3F/R primer pair. Lmna^+, Lmna^fflox, or Lmna^flox allele generates 470, 2114, or 598 bp PCR fragments, respectively. Asterisks mark nonspecific bands (F and G). Primer pairs used and genotypes for Lmna are indicated at the top of the panels (E–G). The relative positions of PCR primers in the Lmna alleles are indicated in A. wt or +; wild-type, ff; fflox, f; flox.
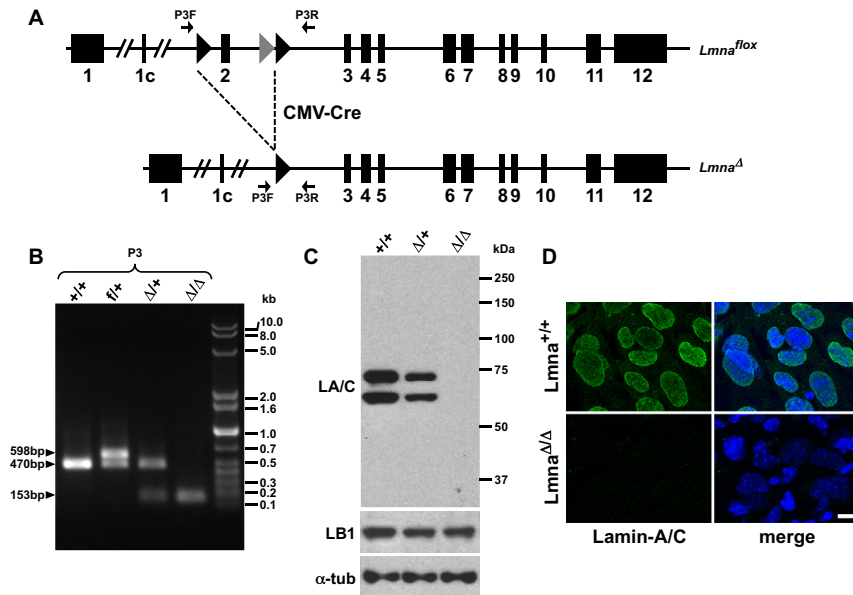
Fig. 2. (A) Strategy to cleave exon 2 of *Lmna* flanked by loxP sites in the *Lmna*flox allele. To delete exon 2 in all tissues including germ cells, *Lmna*flox/+ mice were bred with a mouse strain that expresses Cre recombinase under control of the CMV promoter. Large black and gray arrow heads represent the loxP and Frt sites, respectively. (B) PCR genotyping of *Lmna*+/+, *Lmna*flox/+, *Lmna*Δ/+, and *Lmna*Δ/Δ mice with the P3F/R primer pair. *Lmna*+, *Lmna*flox, or *Lmna*Δ allele generates 470, 598 or 153 bp PCR fragments, respectively. (C) Western blotting analysis of MEFs. LA/C; lamin-A/C, LB1; lamin-B1, α-tub; α-tubulin. Genotypes for *Lmna* are indicated at the top of the panel. (D) Immunofluorescence staining of MEFs with lamin-A/C antibody (left). Lamin-A/C plus DNA staining (right). Scale bar, 10 μm.

examine germline transmission of the *Lmna*fflox allele. The presence of the *Lmna*fflox allele in agouti F1 mice was verified by long-range PCR of tail DNA using the P1F/R and P2F/R primer pairs (Fig. 1E and F). To generate the *Lmna*flox allele in which the puromycin cassette flanked by Frt sites is cleaved, *Lmna*fflox/+ mice were bred with ACTB-FLPe mice, which express FLP1 recombinase under the control of the human β-actin promoter (Fig. 1D). The *Lmna*flox/+ offspring in the next generation were identified by PCR of the flanking regions of exon 2 of *Lmna* using the P3F/R primer pair (Fig. 1G). To generate homozygous *Lmna*flox/flox mice, *Lmna*flox/+ mice were intercrossed. We found that both *Lmna*flox/+ and *Lmna*flox/flox mice were viable and fertile, and did not display any recognizable phenotypes, suggesting that the *Lmna*flox allele does not lead to gain or loss of functions.

3.2. Generation of Lmna^Δ/+ and Lmna^Δ/Δ mice

To examine whether the *Lmna*flox allele generates a loss-of-function allele for *Lmna* upon the expression of Cre recombinase, we set out to analyze *Lmna*Δ/Δ mice in which the 357 bp fragment including exon 2 of *Lmna* is deleted in the entire animals. To create the *Lmna*Δ allele, *Lmna*flox/+ mice were bred with CMV-Cre mice that express Cre recombinase under control of the CMV promoter in all tissues including the germ cells (Fig. 2A). PCR of tail DNA with the primer pair P3F/R confirmed the generation of the *Lmna*Δ allele in the F1 generation of *Lmna*flox/+ × CMV-Cre mating pairs (Fig. 2B). The CMV-Cre allele was then removed by breeding to ensure stable transmission of the *Lmna*Δ allele to the next generation in the absence of CMV-Cre. Heterozygous *Lmna*Δ/+ mice were phenotypically normal and fertile. We intercrossed *Lmna*Δ/+ mice to generate homozygous *Lmna*Δ/Δ mice. In *Lmna*Δ/Δ mice deleted of both copies of exon 2, exon 1 or 1c may undergo cryptic splicing with remaining downstream exons, generating chimeric proteins. We examined this possibility by Western blotting with an antibody raised against the C-terminus of lamin-A proteins. Cell lysates prepared from mouse embryonic fibroblasts (MEFs) indicated that the *Lmna*Δ/Δ cells expressed neither intact nor truncated forms of

lamin-A/C proteins (Fig. 2C). Loss of lamin-A/C in *Lmna*Δ/Δ cells was further confirmed by immunofluorescence staining of MEFs with the anti-lamin-A/C antibody (Fig. 2D). These analyses show that deleting the exon 2 indeed generates a most severe loss-of-function allele for *Lmna* reported to date.

3.3. Lmna^Δ/Δ mice exhibit severe postnatal defects

To further validate whether *Lmna*Δ allele is functionally inactive, we analyzed *Lmna*Δ/Δ mice obtained by intercrossing *Lmna*Δ/+ mice. At birth, pups of all genotypes including *Lmna*Δ/Δ are viable (Table 1) and display no recognizable defect. However, the growth of *Lmna*Δ/Δ mouse was severely retarded after birth compared to *Lmna*+/+ or *Lmna*Δ/+ mice as judged by body weight measurement (Fig. 3A). The body weights of the *Lmna*Δ/Δ mice peaked at around postnatal day 12 and it slightly decreased thereafter. By postnatal day 14 *Lmna*Δ/Δ mice had only ∼53% of the body weight of *Lmna*+/+ or *Lmna*Δ/+ littermates (Fig. 3B). *Lmna*Δ/Δ mice invariably died between postnatal days 16 and 18 (Table 1). These defects of *Lmna*Δ/Δ mice are very similar to those of *Lmna*GT−/− mice reported [13], but are more severe than those of the incomplete *Lmna*Δ8–11/Δ8–11 mice [14].

The germline knockout mice displayed defects in a range of tissues with skeletal muscles being the most severely impaired [13,14]. We did pathology examinations of skeletal muscles to test whether *Lmna*Δ/Δ mice recapitulate the defects of the germline knockout mice reported previously. Immunostaining of skeletal muscle sections from tibialis anterior (TA) confirmed that *Lmna*Δ/Δ mice did not express lamin-A/C (Fig. 3C). Histological

Table 1
Number of animals surviving at the indicated postnatal days.

	P0	P16	P17	P18
Lmna+/+	6	6	6	6
Lmna+/Δ	16	16	16	16
*Lmna*Δ/Δ	10	8	5	0
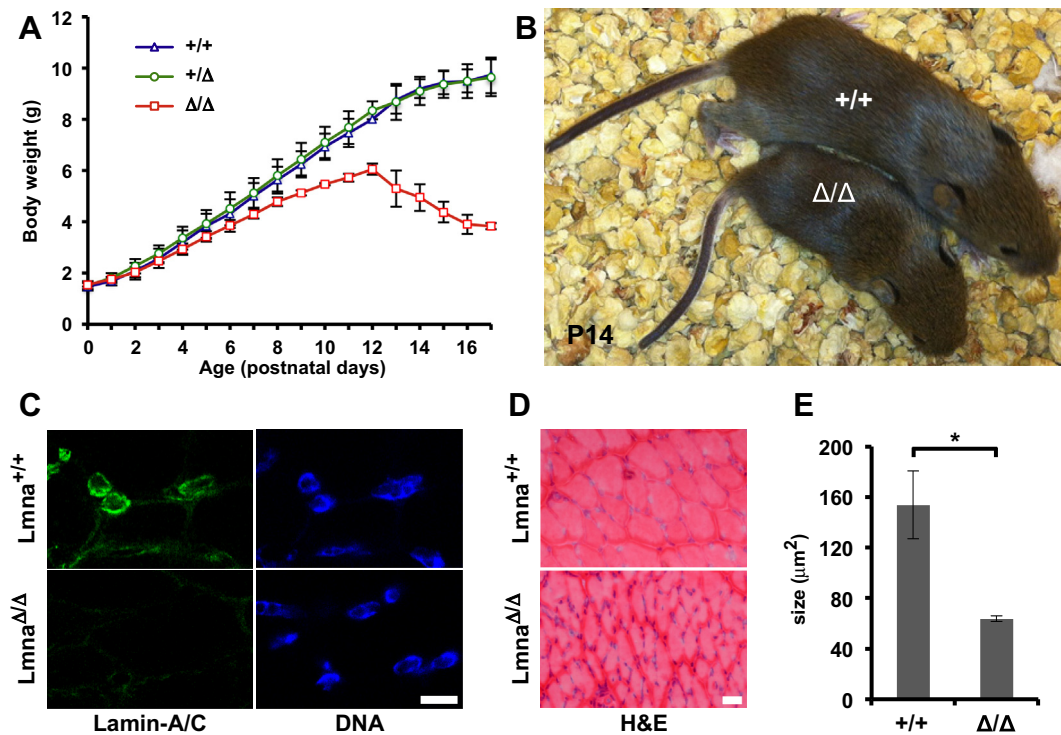
Fig. 3. Characterization of $Lmna^{\Delta/\Delta}$ mice. (A) Body weights of each genotype at indicated postnatal days. (B) Image of 14 day old (P14) mice. (C) Immunofluorescence staining of skeletal muscles with lamin-A/C antibody. Scale bar, 10 µm. (D) H&E staining of skeletal muscles. Scale bar, 20 µm. (E) Quantitation of myofibril size in skeletal muscles. $^*p < 0.05$. Error bars, SD (A and E).

examination of TA muscles revealed that the skeletal myofibrils of $Lmna^{\Delta/\Delta}$ mice are smaller than those of $Lmna^{+/+}$ littermates at postnatal day 15 (Fig. 3D and E). This defect is quite similar to those observed in $Lmna^{GT-/-}$ mice [13]. Together, the above characterizations of $Lmna^{\Delta/\Delta}$ mice show that the $Lmna^{flox}$ allele we have created can be utilized to generate the $Lmna$ loss-of-function allele in spatially and temporally controlled manners.

Conditional knockout alleles are critical for dissecting tissue and cell type specific functions for a given protein. Considering the tissue restricted defects for lamin-A/C mutations, it is critical to decipher the cell-specific functions of lamin-A/C during development and homeostasis. Ideal $Lmna$ conditional alleles should not express any lamin-A/C proteins including truncated isoforms upon Cre expression. Our characterizations show that Cre-mediated deletion of exon 2 of $Lmna$ resulted in no detectable expression of the intact form or C-terminus of lamin-A/C as judged by the available antibodies. We also report that the mice deleted of exon 2 of $Lmna$ are phenotypically similar to $Lmna^{GT-/-}$ mice, which is currently the most severe loss-of-function $Lmna$ mutant [13]. Therefore, the new conditional $Lmna$ knockout mouse and cells reported here provide a great tool to better define lamin-A/C's functions in specific tissues and cell types, which should contribute toward a better understanding of genetic disorders associated with the nuclear lamina. Additionally, by combining with the established conditional knockout mice for lamin-B1 and -B2 [26], it is now possible to deplete all lamins in a spatially and temporally controlled manner in order to define the functions of these important nuclear lamina proteins.

References

[1] B. Burke, L. Gerace, A cell free system to study reassembly of the nuclear envelope at the end of mitosis, Cell 44 (1986) 639–652.

[2] L. Gerace, G. Blobel, The nuclear envelope lamina is reversibly depolymerized during mitosis, Cell 19 (1980) 277–287.

[3] F.D. McKeon, M.W. Kirschner, D. Caput, Homologies in both primary and secondary structure between nuclear envelope and intermediate filament proteins, Nature 319 (1986) 463–468.

[4] G. Krohne, S.L. Wolin, F.D. McKeon, W.W. Franke, M.W. Kirschner, Nuclear lamin LI of *Xenopus laevis*: cDNA cloning, amino acid sequence and binding specificity of a member of the lamin B subfamily, EMBO J. 6 (1987) 3801–3808.

[5] M. Peter, G.T. Kitten, C.F. Lehner, K. Vorburger, S.M. Bailer, G. Maridor, E.A. Nigg, Cloning and sequencing of cDNA clones encoding chicken lamins A and B1 and comparison of the primary structures of vertebrate A- and B-type lamins, J. Mol. Biol. 208 (1989) 393–404.

[6] K. Vorburger, C.F. Lehner, G.T. Kitten, H.M. Eppenberger, E.A. Nigg, A second higher vertebrate B-type lamin. cDNA sequence determination and in vitro processing of chicken lamin B2, J. Mol. Biol. 208 (1989) 405–415.

[7] B. Burke, C.L. Stewart, The nuclear lamins: flexibility in function, Nat. Rev. Mol. Cell Biol. 14 (2013) 13–24.

[8] M.A. Eckersley-Maslin, J.H. Bergmann, Z. Lazar, D.L. Spector, Lamin A/C is expressed in pluripotent mouse embryonic stem cells, Nucleus 4 (2013) 53–60.

[9] R.A. Rober, K. Weber, M. Osborn, Differential timing of nuclear lamin A/C expression in the various organs of the mouse embryo and the young animal: a developmental study, Development 105 (1989) 365–378.

[10] C. Stewart, B. Burke, Teratocarcinoma stem cells and early mouse embryos contain only a single major lamin polypeptide closely resembling lamin B, Cell 51 (1987) 383–392.

[11] G. Bonne, M.R. Di Barletta, S. Varnous, H.M. Becane, E.H. Hammouda, L. Merlini, F. Muntoni, C.R. Greenberg, F. Gary, J.A. Urtizberea, D. Duboc, M. Fardeau, D. Toniolo, K. Schwartz, Mutations in the gene encoding lamin A/C cause autosomal dominant Emery-Dreifuss muscular dystrophy, Nat. Genet. 21 (1999) 285–288.

[12] B.C. Capell, F.S. Collins, Human laminopathies: nuclei gone genetically awry, Nat. Rev. Genet. 7 (2006) 940–952.

[13] N. Kubben, J.W. Voncken, G. Konings, M. van Weeghel, M.M. van den Hoogenhof, M. Gijbels, A. van Erk, K. Schoonderwoerd, B. van den Bosch, V. Dahlmans, C. Calis, S.M. Houten, T. Misteli, Y.M. Pinto, Post-natal myogenic and adipogenic developmental: defects and metabolic impairment upon loss of A-type lamins, Nucleus 2 (2011) 195–207.

[14] T. Sullivan, D. Escalante-Alcalde, H. Bhatt, M. Anver, N. Bhat, K. Nagashima, C.L. Stewart, B. Burke, Loss of A-type lamin expression compromises nuclear

envelope integrity leading to muscular dystrophy, J. Cell Biol. 147 (1999) 913–920.

[15] K.H. Schreiber, B.K. Kennedy, When lamins go bad: nuclear structure and disease, Cell 152 (2013) 1365–1375.

[16] D. Jahn, S. Schramm, M. Schnolzer, C.J. Heilmann, C.G. de Koster, W. Schutz, R. Benavente, M. Alsheimer, A truncated lamin A in the *Lmna*$^{-/-}$ mouse line: implications for the understanding of laminopathies, Nucleus 3 (2012) 463–474.

[17] C.M. Wolf, L. Wang, R. Alcalai, A. Pizard, P.G. Burgon, F. Ahmad, M. Sherwood, D.M. Branco, H. Wakimoto, G.I. Fishman, V. See, C.L. Stewart, D.A. Conner, C.I. Berul, C.E. Seidman, J.G. Seidman, Lamin A/C haploinsufficiency causes dilated cardiomyopathy and apoptosis-triggered cardiac conduction system disease, J. Mol. Cell. Cardiol. 44 (2008) 293–303.

[18] H.J. Worman, Nuclear lamins and laminopathies, J. Pathol. 226 (2012) 316–325.

[19] T.V. Cohen, C.L. Stewart, Fraying at the edge mouse models of diseases resulting from defects at the nuclear periphery, Curr. Top. Dev. Biol. 84 (2008) 351–384.

[20] W.T. Dauer, H.J. Worman, The nuclear envelope as a signaling node in development and disease, Dev. Cell 17 (2009) 626–638.

[21] T. Dechat, K. Pfleghaar, K. Sengupta, T. Shimi, D.K. Shumaker, L. Solimando, R.D. Goldman, Nuclear lamins: major factors in the structural organization and function of the nucleus and chromatin, Genes Dev. 22 (2008) 832–853.

[22] L. Guelen, L. Pagie, E. Brasset, W. Meuleman, M.B. Faza, W. Talhout, B.H. Eussen, A. de Klein, L. Wessels, W. de Laat, B. van Steensel, Domain organization of human chromosomes revealed by mapping of nuclear lamina interactions, Nature 453 (2008) 948–951.

[23] I. Solovei, A.S. Wang, K. Thanisch, C.S. Schmidt, S. Krebs, M. Zwerger, T.V. Cohen, D. Devys, R. Foisner, L. Peichl, H. Herrmann, H. Blum, D. Engelkamp, C.L. Stewart, H. Leonhardt, B. Joffe, LBR and lamin A/C sequentially tether peripheral heterochromatin and inversely regulate differentiation, Cell 152 (2013) 584–598.

[24] S. Wu, G. Ying, Q. Wu, M.R. Capecchi, A protocol for constructing gene targeting vectors: generating knockout mice for the cadherin family and beyond, Nat. Protoc. 3 (2008) 1056–1076.

[25] Y. Kim, A.A. Sharov, K. McDole, M. Cheng, H. Hao, C.M. Fan, N. Gaiano, M.S. Ko, Y. Zheng, Mouse B-type lamins are required for proper organogenesis but not by embryonic stem cells, Science 334 (2011) 1706–1710.

[26] C. Coffinier, H.J. Jung, C. Nobumori, S. Chang, Y. Tu, R.H. Barnes 2nd, Y. Yoshinaga, P.J. de Jong, L. Vergnes, K. Reue, L.G. Fong, S.G. Young, Deficiencies in lamin B1 and lamin B2 cause neurodevelopmental defects and distinct nuclear shape abnormalities in neurons, Mol. Biol. Cell 22 (2011) 4683–4693.